

MOHAMMAD JAVAD NOROOZI *, SEYFOLAH SAEDODIN **, DAVOOD DOMIRI
GANJI ***

NONLINEAR SOLUTION TO A NON-FOURIER HEAT CONDUCTION PROBLEM IN A SLAB HEATED BY LASER SOURCE

The effect of laser, as a heat source, on a one-dimensional finite body was studied in this paper. The Cattaneo-Vernotte non-Fourier heat conduction model was used for thermal analysis. The thermal conductivity was assumed temperature-dependent which resulted in a non-linear equation. The obtained equations were solved using the approximate-analytical Adomian Decomposition Method (ADM). It was concluded that the non-linear analysis is important in non-Fourier heat conduction problems. Significant differences were observed between the Fourier and non-Fourier solutions which stresses the importance of non-Fourier solutions in the similar problems.

1. Introduction

Laser has had increasing and important applications in the recent years. In the industry, laser is employed as a precise manufacturing tool and a concentrated heat source in applications such as cladding, cutting, surface hardening, welding, and machining. In medicine, laser has been utilized as a surgical tool and also for hyperthermia in cancer treatment. Its high temporal and spatial resolution, not involving or heating the unnecessary areas, and the minimal noise has made laser a very popular tool.

Since laser applies a high heat flux in a short period of time, the analysis of laser beam-induced heating is not possible using the classical Fourier's heat conduction law [1-3]. The combination of Fourier's heat conduction

* *PhD of Mechanical Engineering, Young Researchers and Elite Club, Malayer Branch, Islamic Azad University, Malayer, Iran; E-mail: Mo.j.noroozi@gmail.com*

** *Associate Professor, Faculty of Mechanical Engineering, Semnan University, Semnan, Iran; E-mail: s_sadodin@semnan.ac.ir*

*** *Professor, Department of Mechanical Engineering, Babol University of Technology, Babol, Iran, P.O.B. 484; E-mail: mirgang@nit.ac.ir*

law and the energy equation results in a parabolic equation. The parabolic equation leads to the non-physical conclusion which implies an infinite speed of heat propagation. This paradox is not an issue in many common applications. However, the Fourier's law may slightly deviate from exact prediction in applications involving very high heat fluxes [4], heat transfer at very low temperatures [5], and heat transfer at very small scales [6]. For example, Guyer and Krumhansl [7] proved that non-Fourier heat conduction equation is governing in thermal analysis of dielectric crystals at low temperatures. Shirmohammadi [6] analytically investigated the thermal behavior of microspherical particles exposed to laser pulse heating and showed that there is significant deviation between Fourier and non-Fourier results. Tung et al. [4] applied wave heat conduction equation to the laser heating problem of biological tissues and concluded that there are some important differences between Fourier and wave heat conduction models. Therefore, improved models have to be employed in laser heating analysis.

The heat wave model, or the Cattaneo-Vernotte model, is an improved widely-used version of the Fourier's classical model [8], [9]. They defined a thermal relaxation time whose macroscopic description is a time lag between the temperature gradient and the heat flux vector. Another modified model for non-Fourier heat conduction is the Dual Phase Lagging (DPL) model which is first proposed by Tzou [10]. These models have been recently utilized by many researchers. This model was used by Bargmann and Favata [11] to analyze the laser heating in polycrystals. The non-Fourier heat transfer in combined analysis of heat conduction and thermal radiation in a differentially heated 2-D square cavity was studied by Sasmal and Mishra [12]. The non-Fourier heat conduction in a finite slab with insulated boundaries was numerically investigated by Rahbari et al. [13]. An analytical non-Fourier study was conducted by Zhao et al. [14] on a solid sphere under arbitrary surface thermal disturbances. The non-Fourier heat conduction and thermal radiation problem in a concentric spherical shell was studied by Mishra and Sahai [15]. The thermal wave phenomenon in a thin film was analytically examined by Fong and Lam [16].

In most studies on the non-Fourier heat conduction, the equations are linear due to the assumption of constant thermal properties, and nonlinear study of such problems is rare in the literature. The behavior of materials in nature is inherently nonlinear, so the nonlinear study of the mentioned problems is very important in some cases. In the past, in addition to the very limited and difficult analytical methods, numerical methods were used to solve nonlinear problems. These methods were also faced with convergence problem and had a high computational cost. New methods, known as semi-analytical (or approximate-analytical), have recently been proposed for

solving nonlinear problems. Some of the most well-known semi-analytical methods include Adomian Decomposition Method (ADM) [17], Homotopy Perturbation Method (HPM) [18], [19], Homotopy Analysis Method (HAM) [20], Differential Transform Method (DTM) [21], and Variational Iteration Method (VIM) [22].

ADM, which is also used in this study, is one of the most flexible and powerful of these tools that have been employed numerously to solve linear and nonlinear equations. The method was first developed by Adomian [17] and has been used by many researchers. Several applications of this method have been reported recently. Singla and Das [23] used ADM for solving a nonlinear problem involving conductive, convective and radiative stepped fin with temperature-dependent parameters. Duan et al. [24] studied the concentrations of carbon dioxide absorbed into phenyl glycidyl ether using ADM. An analytical solution for the Schrödinger equation for Brownian motion in a double-well potential using ADM was presented by Ai-Jie et al. [25]. Praveen and Rajendran [26] employed ADM and provided a solution to the problem of a reaction-diffusion process involved in packed bed photobioreactor. Fatoorehchi et al. [27] solved the problem of the general RC circuit comprised of a nonlinear resistor in series with a nonlinear capacitor using ADM. ADM was used in another study to solve the problem of Newtonian bio-magneto-tribological squeeze film flow with magnetic induction effects [28].

The application of semi-analytical methods to solve the nonlinear problems of non-Fourier heat conduction problems has been reported just in few studies. Torabi et al. [29] applied the homotopy perturbation method (HPM) to solve a non-linear convective-radiative non-Fourier conduction heat transfer equation with variable specific heat coefficient. Saedodin et al. [30] used the variational iteration method (VIM) to solve the same problem. Differential transformation method (DTM) was applied to analysis of non-linear convective-radiative hyperbolic lumped systems with simultaneous variation of temperature-dependent specific heat and surface emissivity by Torabi et al. [31]. In all of three mentioned references, the governing equations have been only dependent of time and, in fact, ordinary differential equations (ODE) have been solved by semi-analytical methods and, to the best knowledge of the authors, nonlinear partial differential equation (PDE) of non-Fourier heat conduction equation has not been solved yet by semi-analytical methods. However, Srivastava [32] used fractional calculus to explain the wave nature of heat propagation as well as heat conduction at molecular level with dual phase lag model and Modified Adomian Decomposition Method were applied to obtain the approximate analytical solutions of the proposed model. However, it should be noted that an applicable PDE problem must

have boundary conditions, while, in the work of Srivastava [32], there is no boundary conditions.

This study was aimed at investigating the heat transfer in a one-dimensional living tissue subjected to a laser heat source. The non-Fourier heat conduction model was employed for thermal analysis. A nonlinear equation was obtained since the thermal conductivity was assumed temperature-dependent. The obtained equations were solved by ADM. The application of a semi-analytical method such as ADM to solve a system of nonlinear PDEs of non-Fourier heat conduction problem is the novelty and originality of this study.

2. Physical modeling

Figure 1 shows a schematic of the problem geometry. A slab with the thickness $2L$ and the initial temperature $T(x, 0) = \sin(\pi x/2L)$ is insulated on its left side while its right side is at zero temperature. A laser heat flux was considered as a heat source imposed on the left side of the slab. The heat source can be modeled as follows [33-36]:

$$g(x, t) = I_0 \mu (1 - R) e^{-\mu x} (e^{-\beta t} - e^{-\delta t}) \quad (1)$$

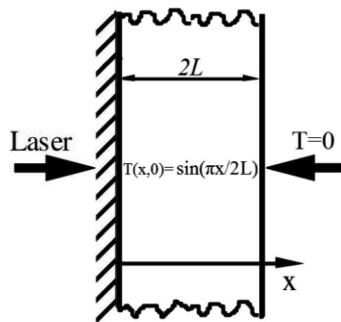


Fig. 1. Schematic of the problem

where $I(t)$ is laser intensity, R is surface reflectance, μ is absorption coefficient, β is laser pulse rise-time parameter, and δ is laser pulse fall-time parameter. The energy conservation equation is as follows:

$$\rho c_p \frac{\partial T(x, t)}{\partial t} + \frac{\partial q(x, t)}{\partial x} - g(x, t) = 0, \quad (2)$$

where ρ is the density of the slab, c_p is specific heat of the slab, $T(x, t)$ is temperature function and $q(x, t)$ is the function of heat flux, x and t are spatial

and temporal variables, respectively. The constitutive equation governing on the problem is based on the thermal wave model [8], [9]:

$$\tau \frac{\partial q(x, t)}{\partial t} + q(x, t) + k \frac{\partial T(x, t)}{\partial x} = 0, \quad (3)$$

where τ is the thermal relaxation time and k is thermal conductivity. Thermal conductivity was assumed a linear function of temperature [37]:

$$k = k_0 [1 + \lambda(T(x, t) - T_0)]. \quad (4)$$

The following parameters were introduced to make the equations (2) and (3) dimensionless:

$$\begin{aligned} \tilde{x} &= \frac{x}{2L}, \quad \tilde{T}(\tilde{x}, Fo) = \frac{T(x, t) - T_0}{T_0}, \quad \alpha_0 = \frac{k_0}{\rho C_p}, \quad c_0^2 = \frac{\alpha_0}{\tau}, \\ \tilde{g}(\tilde{x}, Fo) &= \frac{2L^2 g(x, t)}{T_0 k_0}, \quad Ve^2 = \frac{\alpha_0 \tau}{L^2}, \quad \tilde{\beta} = \frac{2\alpha_0 \beta}{c_0^2}, \quad \tilde{\delta} = \frac{2\alpha_0 \delta}{c_0^2}, \\ \tilde{\mu} &= 2c_0 \tau \mu, \quad Fo = \frac{\alpha_0 t}{2L^2}, \quad \tilde{q}(\tilde{x}, Fo) = \frac{\alpha_0 q(x, t)}{T_0 k_0 c_0}, \quad \gamma = \lambda T_0, \\ g_0 &= \frac{2L^2 I_0 \mu (1 - R)}{k_0 T_0}, \quad \tilde{g}(\tilde{x}, Fo) = g_0 e^{-\mu \tilde{x}} (e^{-\tilde{\beta} Fo} - e^{-\tilde{\delta} Fo}). \end{aligned} \quad (5)$$

The dimensionless form of the equations (2) and (3) are as follows:

$$\frac{\partial \tilde{T}(\tilde{x}, Fo)}{\partial Fo} + \frac{1}{Ve} \frac{\partial \tilde{q}(\tilde{x}, Fo)}{\partial \tilde{x}} - g_0 e^{-\mu \tilde{x}} (e^{-\tilde{\beta} Fo} - e^{-\tilde{\delta} Fo}) = 0 \quad (6)$$

$$Ve^2 \frac{\partial \tilde{q}(\tilde{x}, Fo)}{\partial Fo} + 2\tilde{q}(\tilde{x}, Fo) + Ve [1 + \gamma \tilde{T}(\tilde{x}, Fo)] \frac{\partial \tilde{T}(\tilde{x}, Fo)}{\partial \tilde{x}} = 0. \quad (7)$$

The dimensionless boundary and initial conditions are as follows:

$$\tilde{q}(0, Fo) = 0, \quad \tilde{T}(1, Fo) = 0, \quad \tilde{T}(\tilde{x}, 0) = \sin(\pi \tilde{x}), \quad \tilde{q}(\tilde{x}, 0) = 0. \quad (8)$$

It should be noted that the reason the conditions were chosen in this paper is to demonstrate the flexibility of the ADM, which can easily be adapted to any initial or boundary condition.

3. The basic idea of ADM

Consider a general nonlinear differential equation in the following form:

$$Lu + Ru + Nu = g, \quad (9)$$

where L is the highest-order invertible derivative, R is a linear differential operator with an order less than L , Nu includes the nonlinear terms, and g is the nonhomogeneous term. By applying the inverse operator L^{-1} to both sides of equation (9) and using the given conditions, we have:

$$u = -L^{-1}(Ru) - L^{-1}(Nu) + L^{-1}(g). \quad (10)$$

For nonlinear differential equations, the nonlinear operator $Nu = F(u)$ is expressed by an infinite series called the Adomian polynomials:

$$F(u) = \sum_{m=0}^{\infty} A_m. \quad (11)$$

For A_m polynomials, A_0 depends only on u_0 , A_1 depends only on u_0 and u_1 , A_2 depends only on u_0 , u_1 , and u_2 and so on. ADM provides the solution as follows:

$$u = \sum_{m=0}^{\infty} u_m. \quad (12)$$

For $F(u)$, the infinite series is a Taylor series about u_0 as:

$$F(u) = F(u_0) + F'(u_0)(u - u_0) + F''(u_0)\frac{(u - u_0)^2}{2!} + F'''(u_0)\frac{(u - u_0)^3}{3!} + \dots \quad (13)$$

By rewriting the equation (12) in the form of $u - u_0 = u_1 + u_2 + u_3 + \dots$, and substitution in equation (13) and equating the two terms for $F(u)$ in equation (11) and (13), the relations for the Adomian polynomials are obtained in the following form:

$$\begin{aligned} F(u) &= A_0 + A_1 + A_2 + \dots = \\ &= F(u_0) + F'(u_0)(u_1 + u_2 + \dots) + F''(u_0)\frac{(u_1 + u_2 + \dots)^2}{2!} + \dots \end{aligned} \quad (14)$$

By equating the terms of the above equation, the initial polynomials of the Adomian polynomials are obtained as follows:

$$A_0 = F(u_0), \quad (15)$$

$$A_1 = u_1 F'(u_0), \quad (16)$$

$$A_2 = u_2 F'(u_0) + \frac{1}{2!} u_1^2 F''(u_0), \quad (17)$$

$$A_3 = u_3 F'(u_0) + u_1 u_2 F''(u_0) + \frac{1}{3!} u_1^3 F'''(u_0), \quad (18)$$

$$A_4 = u_4 F'(u_0) + \left(\frac{1}{2!} u_2^2 + u_1 u_3 \right) F''(u_0) + \frac{1}{2!} u_1^2 u_2 F'''(u_0) + \frac{1}{4!} u_1^4 F^{(iv)}(u_0). \quad (19)$$

Now that the (A_m) are obtained, the terms of equation (12) (i.e., the solution to the problem) are determined by inserting the equation (11) into equation (10).

4. Application and modification of ADM

One of the shortcomings of semi-analytical methods, including ADM, in solving PDE is that they are unable of considering the boundary conditions in the solution process [38]. Therefore, ADM has to be improved so that it can include the boundary conditions, and consequently, obtain the correct solution. The method proposed by Olivares [39] for ADM improvement was used here.

According to equation (9), equation (6) and (7) can be rewritten as follows:

$$L_1 = -R_1 + g, \quad (20)$$

$$L_2 = -R_2 - N. \quad (21)$$

Then, the operators introduced in equations (20) and (21) are as follows:

$$\begin{aligned} L_1 &= \frac{\partial \tilde{T}(\tilde{x}, Fo)}{\partial Fo}, & R_1 &= \frac{1}{Ve} \frac{\partial \tilde{q}(\tilde{x}, Fo)}{\partial \tilde{x}}, & g &= g_0 e^{-\tilde{\mu}\tilde{x}} (e^{-\tilde{\beta}Fo} - e^{-\tilde{\delta}Fo}), \\ L_2 &= \frac{\partial \tilde{q}(\tilde{x}, Fo)}{\partial Fo}, & R_2 &= \frac{2}{Ve^2} \tilde{q}(\tilde{x}, Fo) + \frac{1}{Ve} \frac{\partial \tilde{T}(\tilde{x}, Fo)}{\partial \tilde{x}}, \\ N &= \frac{\gamma}{Ve} \tilde{T}(\tilde{x}, Fo) \frac{\partial \tilde{T}(\tilde{x}, Fo)}{\partial \tilde{x}}. \end{aligned} \quad (22)$$

Once the given operators are determined, the values of $\tilde{T}(\tilde{x}, Fo)$ and $\tilde{q}(\tilde{x}, Fo)$ can be obtained according to equation (10). However, since the integration is performed in the Fo direction, the boundary conditions are taken into account at any stage of the solution process, which causes the solution to have errors compared to the accurate solution [38]. Therefore, the method proposed by Olivares [39] was then used to provide the solution.

Two perturbation functions were added to the initial conditions:

$$\tilde{q}^*(\tilde{x}, 0) = p_1(\tilde{x}), \quad (23)$$

$$\tilde{T}^*(\tilde{x}, 0) = \sin(\pi\tilde{x}) + p_2(\tilde{x}). \quad (24)$$

Let the solution be in the form of $\tilde{T} = \tilde{T}_0 + \tilde{T}_1 + \tilde{T}_2 + \dots$ and $\tilde{q} = \tilde{q}_0 + \tilde{q}_1 + \tilde{q}_2 + \dots$. Then, the functions \tilde{T}_0 and \tilde{q}_0 will be in the form of $\tilde{q}_0 = p_1(\tilde{x})$ and

$\tilde{T}_0 = \sin(\pi\tilde{x}) + p_2(\tilde{x})$. The values of other terms are obtained successively using these two functions. Finally, the solution to the problem is obtained by summing all the terms.

After obtaining the solution, the values of the function at the boundary are determined, e.g., $\tilde{q}^*(0, Fo)$ and $\tilde{T}^*(1, Fo)$. These values are certainly different from the boundary conditions of equation (8). The distance between the initial values and the new values has to be minimized at this stage. For this purpose, the distance between the new values and the values in equation (8) are defined as follows:

$$\begin{aligned}
 d[\tilde{q}^*(0, Fo), \tilde{q}(0, Fo)] &= \int_0^1 (\tilde{q}^*(0, Fo) - \tilde{q}(0, Fo))^2 dFo, \\
 d[\tilde{T}^*(1, Fo), \tilde{T}(1, Fo)] &= \int_0^1 (\tilde{T}^*(1, Fo) - \tilde{T}(1, Fo))^2 dFo, \\
 d[\tilde{q}^*(\tilde{x}, 0), \tilde{q}(\tilde{x}, 0)] &= \int_0^1 p_1(\tilde{x})^2 d\tilde{x}, \\
 d[\tilde{T}^*(\tilde{x}, 0), \tilde{T}(\tilde{x}, 0)] &= \int_0^1 p_2(\tilde{x})^2 d\tilde{x}.
 \end{aligned} \tag{25}$$

For the minimization problem, the bulk distance is now expressed as follows:

$$\begin{aligned}
 d &= d[\tilde{q}^*(0, Fo), \tilde{q}(0, Fo)] + d[\tilde{T}^*(1, Fo), \tilde{T}(1, Fo)] + \\
 &+ d[\tilde{q}^*(\tilde{x}, 0), \tilde{q}(\tilde{x}, 0)] + d[\tilde{T}^*(\tilde{x}, 0), \tilde{T}(\tilde{x}, 0)].
 \end{aligned} \tag{26}$$

To minimize the above expression, the forms of the perturbation functions $p_1(\tilde{x})$ and $p_2(\tilde{x})$ have to be known. The most common option is to select a polynomial form:

$$p_1(\tilde{x}) = a_0 + a_1\tilde{x} + a_2\tilde{x}^2 + \dots, \quad p_2(\tilde{x}) = b_0 + b_1\tilde{x} + b_2\tilde{x}^2 + \dots \tag{27}$$

Once the forms of the perturbation functions $p_1(\tilde{x})$ and $p_2(\tilde{x})$ are known, the coefficients $a_0, a_1, a_2, \dots, b_0, b_1, b_2, \dots$ can be obtained through minimization of equation (26). Consequently, the values of perturbation functions $p_1(\tilde{x})$ and $p_2(\tilde{x})$ are obtained thereby yielding the problem solution, i.e. $\tilde{T}(\tilde{x}, Fo)$ and $\tilde{q}(\tilde{x}, Fo)$.

5. Results and discussion

To evaluate the accuracy of the obtained solution, the results were compared to the results of Lam and Fong [40], which is a linear analytical study

(Fig. 2). Figure 2a and Fig. 2b show the temperature profile for $FO = 0.1$ and $FO = 0.5$, respectively. Other parameters were initialized based on the values in Lam and Fong [40] ($g_0 = 100$, $\tilde{\mu} = 5$, $\tilde{\beta} = 1$, $\tilde{\delta} = 5$). Under these conditions, the bulk distance and the perturbation functions coefficients are as follows:

$$\begin{aligned}
 d &= 0.00035, \quad a_0 = -0.01191411095729, \quad a_1 = 0.08909826408173, \\
 a_2 &= -0.1591457465979, \quad a_3 = 0.1171560861847, \quad a_4 = -0.0526205618035, \\
 a_5 &= 0.01061939647927, \quad b_0 = 0.00670551494579, \quad b_1 = 0.04805013071037, \\
 b_2 &= -0.3308149857957, \quad b_3 = 0.1703336781842, \quad b_4 = 0.4320798790908, \\
 b_5 &= -0.2923371327660.
 \end{aligned}$$

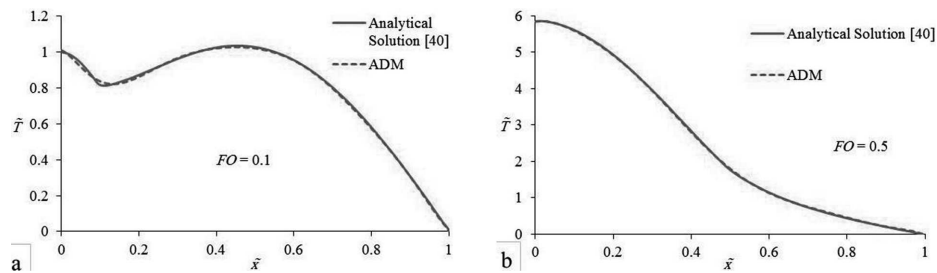


Fig. 2. Validation of ADM with an analytical study [40] ($Ve = 1$, $\gamma = 0$)

As can be seen in the figures, there is a good agreement between the results of the analytical solution and the results obtained from ADM. Quantitatively, ADM has a 0.67% error in Fig. 2a and 0.83% error in Fig. 2b compared to the analytical solution. In both graphs, the behavior of ADM is consistent with the analytic solution. The only inconsistency is that in Fig. 2a, ADM predicts the relative minimum of the graph with a slight distance from the exact location.

5.1. Variations in Vernotte number

The effects of variations in Vernotte number on temperature profile is shown in Fig. 3. In the early parts of the body, an increased Vernotte number increases temperature. This behavior is almost opposite in the endpoints. An increased Vernotte number extends the range of temperature variations and the thermal behavior of the material changes from an exponential behavior (which represents the Fourier heat conduction) to the wavelike behavior (which represents the non-Fourier heat conduction). This behavior is due to the nature of the Vernotte number ($Ve^2 = \frac{\alpha_0 \tau}{L^2}$). Greater relaxation times,

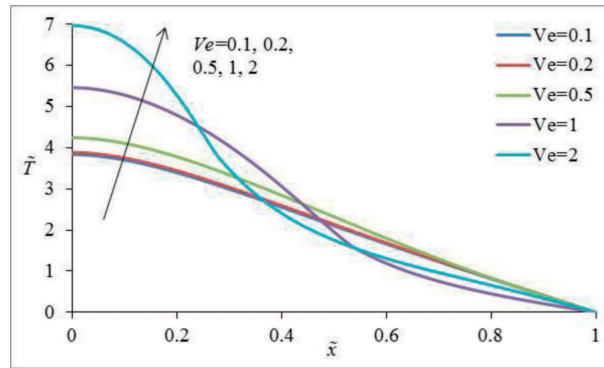


Fig. 3. The effect of Vernotte number on temperature profiles ($Fo = 0.5, \gamma = 0.1$)

and consequently greater Vernotte numbers, show the greater tendency of the body to deviate from the Fourier heat conduction.

5.2. Variations in thermal conductivity coefficient (γ)

The effects of variations in thermal conductivity coefficient on temperature profile are shown in Fig. 4. If the body is divided into three parts, in its first one-third, an increased γ decreases temperature. In the middle one-third, increase in γ increases the temperature. In the final one-third, the diagrams converge to each other. Lower values of γ lead to greater temperature gradient as well as greater surface temperature, and vice versa, i.e., larger γ leads to smaller temperature gradient and surface temperatures. Thus, by increasing γ , the diagrams show different behaviors. Since the heat source is spatially-decaying, the thermal energy is dissipated at the end of the body, and the diagrams converge to each other.

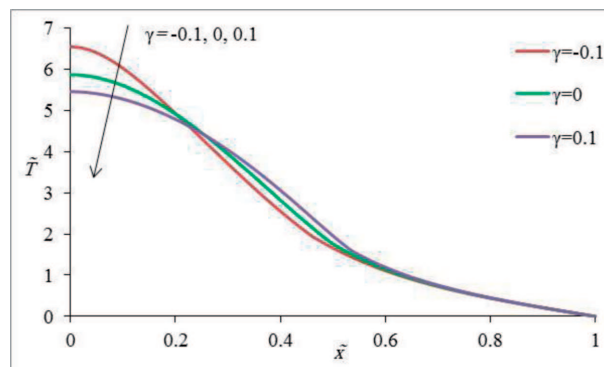


Fig. 4. The effect of γ on temperature profiles ($Ve = 1, Fo = 0.5$)

5.3. Variations in Fourier number

Figure 5 shows the effects of variations in Fourier number. In the early parts of the body, increasing the Fourier number at a given point increases the temperature which is due to the increased heat source energy. Since the Fourier number represents the dimensionless time, at very low Fourier numbers, the temperature initial condition $[\tilde{T}(\tilde{x}, 0) = \sin(\pi\tilde{x})]$ is dominant in the form of a sine wave in the background of temperature distribution. Over time, the effects of heat source appear, and the wave-like behavior caused by non-Fourier heat conduction is gradually observed in areas close to the surface. At the endpoints, the diagrams converge to each other due to the nature of the heat source discussed in the previous figure.

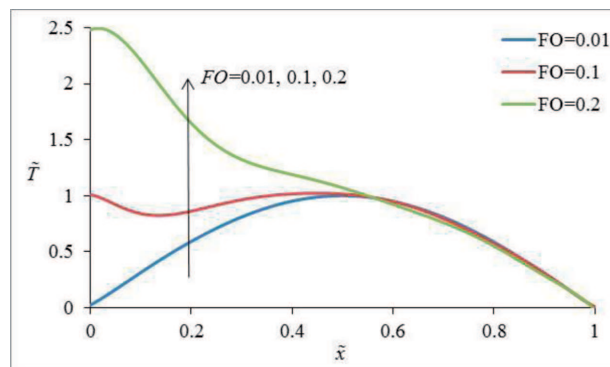


Fig. 5. The effect of Fourier number on temperature profiles ($Ve = 1$, $\gamma = 0.1$)

5.4. The effects of Fourier and non-Fourier heat conduction

A comparison was performed between the solution of the Fourier model and the solution of the non-Fourier model. Figure 6 shows the comparison between the two values of γ . In the diagrams of the nonlinear case, we have $\gamma = 0.5$. The results are interesting. There are significant differences between Fourier and non-Fourier solutions, and the variation gradient is greater in the non-Fourier solution compared to the Fourier one. In the initial points of the body, the non-Fourier solution takes greater values, and then, since it has a steeper decreasing slope compared to the Fourier solution, the two solutions coincide. After that, the Fourier solution has a greater value than the non-Fourier one. In addition, Fig. 6 shows that the effect of non-linear equations is more visible in the non-Fourier case. The diagrams in fact show that in cases where the non-Fourier model should be used, the use of Fourier model would have unacceptably large errors. Also assuming a constant thermal

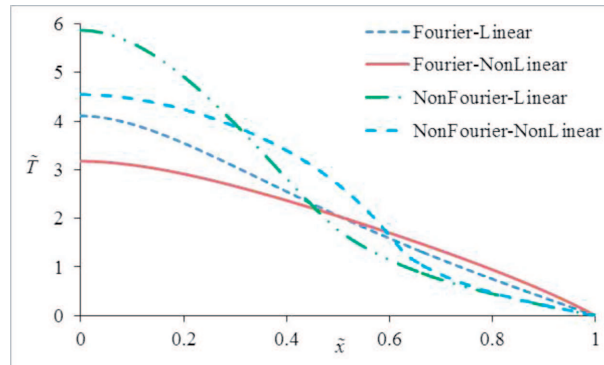


Fig. 6. The comparison between Fourier and non-Fourier solutions for linear and nonlinear cases ($Ve = 1$, $Fo = 0.5$, Linear: $\gamma = 0$, NonLinear: $\gamma = 0.5$)

conductivity (especially in the non-Fourier case) causes the results to have large error.

5.5. Sensitivity analysis

In this section, the sensitivity of the dimensionless temperature to the variations in various parameters of the problem is analyzed. Figure 7 shows the percentage change in temperature versus the percentage changes in various parameters. The variations in the Fourier number (or the dimensionless time) have the greatest effect on the temperature while the variations in γ and Vernotte number have the least effect on the temperature. The heat source parameters are also included among them. This result was expected, because the non-Fourier heat conduction problems are extremely time-dependent, and

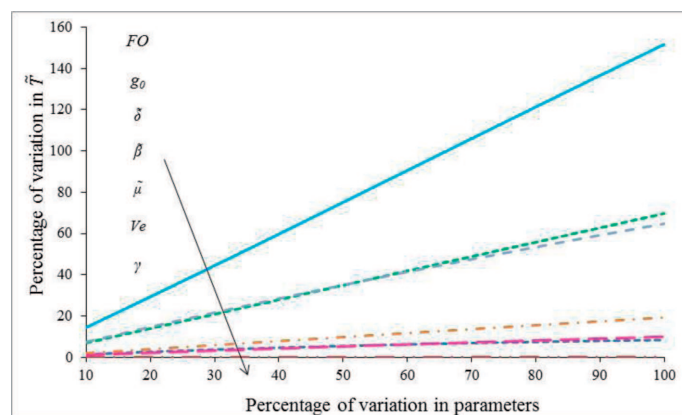


Fig. 7. Sensitivity analysis of the dimensionless temperature at $\tilde{x} = 0$ with respect to different parameters (Reference values: $Ve = 1$, $\gamma = 0.1$, $Fo = 0.1$, $g_0 = 100$, $\mu = 5$, $\beta = 1$, $\delta = 5$)

t	time (s)	ρ	density (kgm^{-3})
Ve	Vernotte number	τ	relaxation time (s)

Manuscript received by Editorial Board, September 29, 2015;
 final version, December 23, 2015.

REFERENCES

- [1] Özişik M.N., Tzou D.Y.: On the Wave Theory in Heat Conduction. *J. Heat Transfer*, 1994, Vol. 116, No. 3, pp. 526-535.
- [2] Tang D.W., Araki N.: Wavy, wavelike, diffusive thermal responses of finite rigid slabs to high-speed heating of laser-pulses. *Int. J. Heat Mass Transf.*, 1999, Vol. 42, No. 5, pp. 855-860.
- [3] Wang X., Xu X.: Thermoelastic wave in metal induced by ultrafast laser pulses. *J. Therm. Stress.*, 2002, Vol. 25, No. 5, pp. 457-473.
- [4] Tung M.M., Trujillo M., López Molina J., Rivera M.J., Berjano E.J.: Modeling the heating of biological tissue based on the hyperbolic heat transfer equation. *Math. Comput. Model.*, 2009, Vol. 50, No. 5-6, pp. 665-672.
- [5] Peshkov V.: Second Sound in Helium II. *J. Physics, USSR*, 1944, Vol. 3, p. 381.
- [6] Shirmohammadi R.: Thermal Response of Microparticles Due to Laser Pulse Heating. *Nanoscale Microscale Thermophys. Eng.*, 2011, Vol. 15, No. 3, pp. 151-164.
- [7] Guyer R.A., Krumhansl J.A.: Solution of the Linearized Phonon Boltzmann Equation. *Phys. Rev.*, Aug. 1966, Vol. 148, No. 2, pp. 766-778.
- [8] Cattaneo C.: A form of heat conduction equation which eliminates the paradox of instantaneous propagation. *Comput. rendus*, 1958, Vol. 247, pp. 431-433.
- [9] Vernotte P.: Some possible complications in the phenomenon of thermal conduction *Comput. rendus*, 1961, Vol. 247, pp. 2190-2191.
- [10] Tzou D.Y.: A Unified Field Approach for Heat Conduction From Macro- to Micro-Scales. *J. Heat Transfer*, 1995, Vol. 117, No. 1, pp. 8-16.
- [11] Bargmann S. Favata A.: Continuum mechanical modeling of laser-pulsed heating in polycrystals: A multi-physics problem of coupling diffusion, mechanics, and thermal waves. *ZAMM – J. Appl. Math. Mech. / Zeitschrift für Angew. Math. und Mech.*, 2014, Vol. 94, No. 6, pp. 487-498.
- [12] Sasmal A., Mishra S.C.: Analysis of non-Fourier conduction and radiation in a differentially heated 2-D square cavity. *Int. J. Heat Mass Transf.*, 2014, Vol. 79, pp. 116-125.
- [13] Rahbari I., Mortazavi F., Rahimian M.H.: High order numerical simulation of non-Fourier heat conduction: An application of numerical Laplace transform inversion. *Int. Commun. Heat Mass Transf.*, 2014, Vol. 51, pp. 51-58.
- [14] Zhao W.T., Wu J.H., Chen Z.: Analysis of non-Fourier heat conduction in a solid sphere under arbitrary surface temperature change. *Arch. Appl. Mech.*, 2014, Vol. 84, No. 4, pp. 505-518.
- [15] Mishra S.C., Sahai H.: Analysis of non-Fourier conduction and volumetric radiation in a concentric spherical shell using lattice Boltzmann method and finite volume method. *HEAT MASS Transf.*, 2014, Vol. 68, pp. 51-66.
- [16] Fong E., Lam T.T.: Asymmetrical collision of thermal waves in thin films: An analytical solution. *Int. J. Therm. Sci.*, 2014, Vol. 77, pp. 55-65.
- [17] Adomian G.: *Stochastic Systems*. New York, Academic Press, 1983.
- [18] He J.: An approximate solution technique depending on an artificial parameter: A special example. *Commun. Nonlinear Sci. Numer. Simul.*, 1998, Vol. 3, No. 2, pp. 92-97.

- [19] He J.: Newton-like iteration method for solving algebraic equations. *Commun. Nonlinear Sci. Numer. Simul.*, 1998, Vol. 3, No. 2, pp. 106-109.
- [20] Liao S.J.: *The proposed homotopy analysis technique for the solution of nonlinear problems.* Tong University, 1992.
- [21] Zhou J.K.: *Differential Transform and Its Applications for Electrical Circuits.* Huarjung University Press, 1986.
- [22] He J.: Variational iteration method – a kind of non-linear analytical technique: some examples. 1999, Vol. 34, pp. 699-708.
- [23] Singla R.K., Das R.: Adomian decomposition method for a stepped fin with all temperature-dependent modes of heat transfer. *Int. J. Heat Mass Transf.*, 2015, Vol. 82, No. 0, pp. 447-459.
- [24] Duan J.-S., Rach R., Wazwaz A.-M.: Steady-state concentrations of carbon dioxide absorbed into phenyl glycidyl ether solutions by the Adomian decomposition method. 2014, *J. Math. Chem.*, pp. 1-14.
- [25] Liu A.-J., Zheng L.-C., Ma L.-X., Zhang X.-X.: Analytical Solutions of a Model for Brownian Motion in the Double Well Potential. *Commun. Theor. Phys.*, 2015, Vol. 63, No. 1, p. 51-56.
- [26] Praveen T., Rajendran L.: Theoretical analysis through mathematical modeling of two-phase flow transport in an immobilized-cell photobioreactor. *Chem. Phys. Lett.*, 2015, Vol. 625, pp. 193-201.
- [27] Fatoorehchi H., Abolghasemi H., Zarghami R.: Analytical approximate solutions for a general nonlinear resistor-nonlinear capacitor circuit model. *Appl. Math. Model.*, 2015, Vol. 39, No. 19, pp. 6021-6031.
- [28] Bég O.A., Tripathi D., Sochi T., Gupta P.K.: Adomian Decomposition Method (ADM) simulation of magneto-bio-tribological squeeze film with magnetic induction effects. *J. Mech. Med. Biol.*, 2015, Vol. 15, No. 5, p. 1550072.
- [29] Torabi M., Yaghoobi H., Saedodin S.: Assessment of homotopy perturbation method in non-linear convective-radiative non-Fourier conduction. *Therm. Sci.*, 2011, Vol. 15, pp. 263-274.
- [30] Saedodin S., Yaghoobi H., and Torabi M.: Application of the variational iteration method to nonlinear non-Fourier conduction heat transfer equation with variable coefficient. 2011, Vol. 40, No. 6, pp. 513-523.
- [31] Torabi M., Yaghoobi H., Boubaker K.: Thermal Analysis of Non-linear Convective – Radiative Hyperbolic Lumped Systems with Simultaneous Variation of Temperature-Dependent Specific Heat and Surface Emissivity by MsDTM and BPES. *Int. J. Thermophys.*, 2013, Vol. 34, No. 1, pp. 122-138.
- [32] Srivastava V.: Dual-phase-lag heat equation of fractional order of heat transfer within microscale region. *World J. Model. Simul.*, 2013, Vol. 9, No. 3, pp. 216-222.
- [33] Yilbas B.S.: A closed form solution for temperature rise inside solid substrate due to time exponentially varying pulse. *Int. J. Heat Mass Transf.*, 2002, Vol. 45, No. 9, pp. 1993-2000.
- [34] Cheung T.-Y.K., Blake B.A., Lam T.T.: Heating of Finite Slabs Subjected to Laser Pulse Irradiation and Convective Cooling. *J. Thermophys. Heat Transf.*, 2007, Vol. 21, No. 2, pp. 239-323.
- [35] Fong E., Lam T., Davis S.: *Heat Transfer in Isotropic and Orthotropic Materials Subjected to Laser Irradiation and Radiative Cooling.* 40th Thermophysics Conference, American Institute of Aeronautics and Astronautics, 2008.
- [36] Lam T.T.: Thermal propagation in solids due to surface laser pulsation and oscillation. *Int. J. Therm. Sci.*, 2010, Vol. 49, No. 9, pp. 1639-1648.
- [37] Malekzadeh P., Rahideh H.: IDQ two-dimensional nonlinear transient heat transfer analysis of variable section annular fins, *Energy Convers. Manag.*, 2007, Vol. 48, No. 1, pp. 269-276.
- [38] Biazar J., Islam M.R.: The Adomian Decomposition Method for the solution of the transient energy equation in rocks subjected to laser irradiation. *Iran. J. Sci. Technol. Trans. A*, 2006, Vol. 30, No. A2, pp. 201-212.

- [39] García-Olivares A.: Analytic solution of partial differential equations with Adomian's decomposition, *Kybernetes*, 2003, Vol. 32, No. 3, pp. 354-368.
- [40] Lam T.T., Fong E.: Heat diffusion vs . wave propagation in solids subjected to exponentially-decaying heat source: Analytical solution. *Int. J. Therm. Sci.*, 2011, Vol. 50, No. 11, pp. 2104-2116.

Nieliniowe rozwiązanie problemu niefourierowskiego przewodzenia ciepła w płycie nagrzewanej źródłem laserowym

Streszczenie

W artykule badano działanie laserowego źródła ciepła na ciało jednowymiarowe o skończonych wymiarach. Do analizy rozkładu temperatury zastosowano niefourierowski model przewodnictwa ciepła Cattaneo-Vernotte. Założono, że przewodność cieplna jest zależna od temperatury, w wyniku czego otrzymano równania nieliniowe. Do rozwiązania równań zastosowano przybliżoną analityczną metodę dekompozycji Adomiana (ADM). Stwierdzono, że analiza nieliniowa ma istotne znaczenie w problemach przewodnictwa ciepła typu niefourierowskiego. Zaobserwowano istotne różnice między rozwiązaniami fourierowskimi i niefourierowskimi, co podkreśla celowość stosowania tych ostatnich w podobnych problemach.